national accelerator laboratory

FERMILAB-Pub-74/103-THY/EXP
7100.186

(Submitted to Phys. Rev. D)

NUCLEON DIFFRACTIVE DISSOCIATION

II. ENERGY DEPENDENCE OF THE LOW MISSING MASS CROSS SECTION AND CONSTRAINTS ON TRIPLE REGGE COUPLINGS

V. A. Tsarev*

October 1974

*Joint Institute for Nuclear Research, Dubna, and P. N. Lebedev Physical Institute, Moscow, USSR.

Operated by Universities Research Association Inc. Under Contract with the United States Atomic Energy Commission

NUCLEON DIFFRACTIVE DISSOCIATION

II. ENERGY DEPENDENCE OF THE LOW MISSING MASS CROSS SECTION AND CONSTRAINTS ON TRIPLE REGGE COUPLINGS

V. A. Tsarev*
Fermi National Accelerator Laboratory, Batavia, Illinois 60510 USA†

ABSTRACT

The energy dependence of the Deck-type model is discussed and shown to be in good agreement with data on the low mass nucleon diffractive dissociation. On the basis of finite mass sum rules relations between triple Regge couplings and different Regge contributions to elastic and Deck amplitudes are obtained and duality for Reggeon-nucleon scattering amplitudes is examined. The normal two-component duality usually assumed for nondiffractive terms is found to be in contradiction with experimental data.

I. INTRODUCTION

Recent measurements of the low mass nucleon diffractive dissociation display the following picture.[1] The most prominent feature of the missing-mass spectrum at small $|t|$ is a broad enhancement with maximum at $M_x \sim 1.4$ GeV. The main contribution to this bump comes from one-pion production channel. On the top of the bump some narrow resonance peaks are superimposed. The integral contribution of these resonance peaks in the low-mass region ($M_x^2 \lesssim 3$ GeV) is much smaller than the contribution of the bump. This is clearly seen in Fig. 1 showing recent ISR results for reaction $pp \to \pi^+ np$.[2] The cross section in the bump region has very steep t-dependence and dies away quickly as $|t|$ grows. As a result at $|t| \gtrsim 0.2$ GeV^2 the resonance contributions become comparable with bump contribution.

In our previous paper[3] we discussed the relevance of the peripheral Drell-Hiida-Deck (DHD)-type model[4] to the nucleon excitation in the region of 1.4 GeV bump. Taking into account absorptive corrections this model was shown to give a reasonable explanation for the main properties of the low mass diffractive dissociation.

In the present paper we shall use this model to obtain some information on high mass nucleon dissociation. One of the possible ways to do so is to assume that the DHD-type diagram retains its importance at high M_x. Then the sum of these diagrams will lead to a pion-triangle model for triple Regge couplings (Fig. 2). However it is hard to believe that DHD-type contributions would be only important at high M_x. Many other contributions may enter the play so we do not expect qualitatively correct results in this approach. The other way is to use DHD model only in the region where it is known to be important, i.e., at low M_x, and connect it with high-mass region by finite mass sum rules (FMSR).[5] The reason for using the model for low mass inelastic scattering rather than the experimental data itself is the following. In order to obtain information on different triple Regge couplings we need to know the contributions of the corresponding Regge exchanges into the low mass inelastic scattering and DHD model predicts it in terms of the presumably known Regge contributions to πN-scattering amplitude. If we want to extract such information directly from the data on inelastic scattering, we need anyhow some model. Moreover it gives predictions even at such values of t where experimental data are still not available, in particular at $t \to 0$[6] which is important for understanding of the small-t behavior of triple Regge couplings. In what follows we shall assume:

(i) Semilocal duality. It means that the FMSR should be valid for low cutoff which we choose at $M_x^2 = 3\ \mathrm{GeV}^2$.

(ii) The whole 1.4 GeV bump will be described by DHD-type model for one-pion production. Two-pion channel can also be easily accommodated in our scheme by $\Delta\pi$-production. Estimation for $\Delta\pi$ gives, however, relatively small ($\lesssim 15\%$) contribution which we shall neglect.

(iii) Guided by experimental data[2] we shall also neglect resonance contributions into sum rule integrals.

The last two approximations are reasonable only at small $|t|$ where 1.4 GeV bump dominates inelastic cross section. So in what follows we shall restrict our consideration to a small $|t|$ region $|t| \leq 0.1$ GeV^2. Then the only terms which contribute to the low-mass integral are the elastic term (which is equivalent to resonance contribution into ordinary FESR) and the DHD-contribution (equivalent of nonresonant background).

In Section II we generalize our previous result for DHD cross section and take into account in a very simple way nondiffractive parts of the DHD amplitude connected with contributions of secondary trajectories into elastic πN scattering. Predicted energy dependence of the 1.4 GeV bump is shown to be in good agreement with experimental data. Then in Section III we obtain equations connecting diffractive and nondiffractive contributions into low- and high-mass regions of the form:

$$\langle E(i,j)\rangle + \langle D(i,j)\rangle = \langle (i,j,P) + (i,j,R)\rangle \begin{cases} i=j=P \\ i=P,\ j=R \\ i=j=R \end{cases} \qquad (1)$$

shown graphically in Fig. 3. Here $\langle E(i,j)\rangle$ and $\langle D(i,j)\rangle$ are integrals over M_x of elastic and DHD terms, corresponding to exchange of α_i and α_j, while (i,j,k) corresponds to triple Regge coupling $G_{i,j,k}$. P is the Pomeron and R is secondary trajectory. These equations can be useful in reducing of the 6 unknown triple Regge terms to only 3. Further information could be obtained if one can separate somehow (i,j,P) and (i,j,R) terms in Eq. (1). For usual two-body hadronic reactions such separation based on Harari-Freund two-component duality[7] is known to work very nicely. It connects the resonance contributions to the FESR with ordinary Regge trajectories, while background with Pomeron. However this "normal" two-component duality cannot be generalized to multibody amplitudes in a straightforward model independent way.[8] It is commonly believed that for non-Pomeron exchanges, i.e., for amplitudes R + h (hadron) → h + R and R + h → P + h normal two-component duality works.[9] For Pomeron-particle amplitudes some arguments were given in favor of "abnormal" duality where resonances in the direct channel build up the Pomeron in the cross channel.[9] Here we shall use the name "abnormal" for the extreme case when the whole resonance contribution is connected with P whereas nonresonant part builds up R. We shall distinguish it from the weaker form which we call "mixed" duality. In this case resonance and background contribute partly to P and R. It is worth to note that the secondary vacuum trajectory f^0 can also share with Pomeron its "abnormal" properties.[11] ρ.

In Section IV these extreme types of duality are examined. Triple Regge couplings obtained from separated equations [Eq. (1)] are compared with experimental data on proton diffractive dissociation.

II. ENERGY DEPENDENCE OF THE LOW MISSING MASS CROSS SECTION

According to our assumptions we shall describe the inclusive cross section for reaction pp → Xp in the region of the 1.4 GeV bump by DHD-type diagrams of Fig. 4. It has been shown in Ref. 3 that at small $|t|$ the absorptive corrections can be effectively taken into account by phenomenological form factors. Then the inclusive cross section can be expressed in terms of πN elastic scattering amplitude $T_{\pi N}$ in a form similar to the traditional DHD model:

$$\left(\frac{d\sigma}{dt\,dM_x^2}\right)_{NN\to\pi NN} = \int_{-1}^{+1} d\cos\theta \int_0^{2\pi} d\phi\ \Phi(s,t,\phi,\theta,\ M_x^2)\,\left|T_{\pi N}(t,s_1)\right|^2 . \quad (2)$$

Here θ and ϕ are polar and azimuthal angles of the incoming nucleon three-momentum in the c. m. of the produced $\pi + N$ system and Φ contains kinematical factors, form factors, and the π-meson propagator. In the high-energy limit, considered in Ref. 3, we took into account only diffractive (Pomeron) contributions and the πN scattering amplitude was approximated by energy independent form $T_{\pi N} = i\,\sigma_{tot}(\pi N)\, e^{b_{\pi N} t}$. If subenergy s_1 of the πN scattering is small, secondary trajectories are also important, and we have:

$$T(\pi^{\pm} p \to \pi^{\pm} p) = P + f \pm \rho \tag{3}$$

$$T(\pi^{o} p \to \pi^{o} p) = P + f, \tag{4}$$

where

$$\begin{aligned} P &= \beta_P(t)\, X_P(t)\, s_1^{\alpha_P(t)-1} \\ f &= \beta_f(t)\, X_f(t)\, s_1^{\alpha_f(t)-1} \\ \rho &= \beta_\rho(t)\, X_\rho(t)\, s_1^{\alpha_\rho(t)-1}. \end{aligned} \tag{5}$$

$\alpha_i(t)$ and $\beta_i(t)$ are trajectories and residues of Regge poles and $X_i(t)$ is a signature factor

$$X_i(t) = \frac{1 + \tau_i e^{-i\pi\alpha_i}}{-\sin \pi\alpha_i} .$$

In what follows we choose $\alpha_\rho(t) = \alpha_f(t) = \alpha_\omega(t) = 1/2 + \alpha_R' t$. The ρ contribution which is responsible for the difference between π^+-, π^--, and π^o-N scattering is known to be relatively small. It can be estimated from the data on $\pi^{\pm} p$ total cross sections:[11]

$$\sigma_{\pi^{\pm}p} = \mathrm{Im}\,(P + f \pm \rho)_{t=o} = 21.3 + (20.35 \mp 4.55)\; s_1^{-1/2}. \qquad (6)$$

Neglecting the ρ contribution we have $T_{\pi^+p} = T_{\pi^o p}$ and together with relations (2)-(5) and $G^2_{\pi^+np} = 2\,G^2_{\pi^o pp}$ it gives

$$\left(\frac{d\sigma}{dtdM_x^2}\right)_{\substack{pp \to Xp \\ \text{near } 1.4\text{ GeV}}} \simeq 3\left(\frac{d\sigma}{dtdM_x^2}\right)_{pp \to \pi^o pp}\,, \qquad (7)$$

where

$$\left(\frac{d\sigma}{dtdM_x^2}\right)_{pp\to\pi^o pp} = \int_{-1}^{+1} d\cos\theta \int_{o}^{2\pi} d\phi\; \Phi(s, t, \theta, \phi, M_x^2)\, e^{b_{\pi N}t}\, \sigma^2_{tot}(\pi N)$$

$$\Big\{ \tilde{\beta}_P(t)\,|X_P(t)|^2\, s_1^{2\alpha_P(t)-2} +$$

$$+ 2\,\tilde{\beta}_P(t)\tilde{\beta}_R(t)\mathrm{Re}\,[X_P^*(t)X_f(t)]\; s_1^{\alpha_P(t)+\alpha_R(t)-2} +$$

$$+ \tilde{\beta}^2_R(t)\,|X_f(t)|^2\, s_1^{2\alpha_R(t)-2} \Big\} \qquad (8)$$

and

$$\tilde{\beta}_i(t) = \frac{\beta_i(t)}{\sigma_{tot}(\pi N)}\, e^{-b_{\pi N}t}. \qquad (9)$$

The subenergy s_1 is connected with total energy s by the following relation:

$$s_1 = A(s) + B(s)\cos\theta + C(s)\sin\theta\cos\phi, \qquad (10)$$

where A, B, and C are known functions of s and M_x.[3] Thus the Eqs. (8) and (10) determine the energy-dependence of the proton excitation cross section in the region of 1.4 GeV bump. In the simple energy independent approximation for $T_{\pi N}^{3}$ we were able to calculate integral (8) analytically. In the general case the integral can be calculated only numerically. However, we can avoid this complication using a simple approximation for Eq. (10). At the threshold $M_x = M_N + \mu$ Eq. (10) reduces to

$$s_1 = s/\lambda, \ \lambda = (M_N + \mu)/\mu \sim 7.7 \tag{11}$$

and we shall use this simple relation in the whole low-mass interval $M_x \lesssim 1.7$ GeV.

One can see from Eq. (11) that even at Fermilab energies s_1 is relatively small leading to the importance of the nondiffractive contributions in the DHD cross section.

Using Eq. (11), Eq. (8) can be rewritten as

$$\left(\frac{d\sigma}{dt dM_x^2}\right)_{pp\to Xp} = \left(\frac{d\sigma}{dt dM_x^2}\right)_0 F(s,t) \tag{12}$$

where

$$F(s,t) = D_{PP}(t)\, s^{2\alpha_P(t)-2} + D_{PR}(t)\, s^{\alpha_P(t) + \alpha_R(t)-2} + D_{RR}(t)\, s^{2\alpha_R(t)-2} \tag{13}$$

and

$$\begin{aligned} D_{PP} &= (\lambda)^{2-2\alpha_P(t)}\, \tilde{\beta}_P^{\,2}(t) |X_P(t)|^2 \\ D_{RP} &= (\lambda)^{2-\alpha_P(t)-\alpha_R(t)}\, \tilde{\beta}_P(t)\, \tilde{\beta}_R(t)\, \mathrm{Re}\, |X_P^*(t)\, X_f(t)| \\ D_{RR} &= (\lambda)^{2-2\alpha_R(t)}\, \tilde{\beta}_R^{\,2}(t) |X_f(t)|^2 . \end{aligned} \tag{14}$$

Let us now compare these formulae with experimental data. We can fix the parameters $\tilde{\beta}_R$ and $\tilde{\beta}_R$ from the data on πN scattering. Parametrizing residue functions by usual exponential expression

$$\beta_i(t) = \beta_i(o)\, e^{b_i t}$$

we take for simplicity $b_P = b_R = b^o_{\pi N}$ and choose the value 6 GeV^{-2} for $b^o_{\pi N}$.[12] From (5) and (6) $\tilde{\beta}_P(o) \sim 0.89$ and $\tilde{\beta}_R(o) \simeq 0.85$. At small $|t|$ the function $F(s,t)$ can be approximated by the following form:

$$F(s,t) \simeq 0.79\, e^{(0.5\ln s - 4)t} + 4.2\, e^{-5.5t + \ln s(-0.5 + 1.25t)} + \\ + 11.1(1-\pi t)\, e^{-7.1t + (2t-1)\ln s}. \qquad (15)$$

Multiplying it by the cross section $(d\sigma/dtdM_x^2)_o$ from Ref. 3, one can find $(d\sigma/dtdM_x^2)_{pp\to Xp}$ at different s values. In Fig. 5 we show the comparison of the calculation for $t = -0.04$ and $M_x = 1.4$ with experimental data.[14] The agreement is good and confirms the validity of the model.

In the next section we shall also need the expression for pp elastic cross section in terms of Regge contributions. Neglecting ρ and A_2 which are known to couple weakly to $N\bar{N}$ we have

$$T_{pp} = P + f + \omega . \qquad (16)$$

Assuming exchange degeneracy for f and ω one can write it as

$$T_{pp} = \gamma_P^2(t)\, s^{\alpha_P(t)-1}\, X_P(t) + \frac{2\gamma_R^2(t)}{\sin \pi\alpha_R(t)}\, s^{\alpha_R(t)-1}, \qquad (17)$$

where $\gamma_i(t)$- is vertex function for pp i coupling.

Then

$$\left(\frac{d\sigma}{dt}\right)_{el} = E_{PP}\, s^{2\alpha_P(t)-2} + E_{PR}\, s^{\alpha_P(t)+\alpha_R(t)-2} + E_{RR}\, s^{2\alpha_R(t)-2}, \quad (18)$$

where

$$E_{PP} = \frac{1}{16\pi}\, \gamma_P^4(t)\, |X_P(t)|^2$$

$$E_{RR} = \frac{1}{16\pi}\, \frac{4\, \gamma_R^4(t)}{\sin^2 \pi\, \alpha_R(t)}$$

$$E_{PR} = \frac{1}{16\pi}\, \frac{4\, \gamma_P^2(t)\, \gamma_R^2(t)}{\sin \pi\, \alpha_R(t)}\, \mathrm{Re}\, X_P(t) \quad (19)$$

are contributions of PP, RR, and the cross term.

From the experimental data on pp and $p\bar{p}$ total cross sections one can find[11] the following values of parameters

$$\gamma_P^2(o) = 37.4 \text{ mb}, \; \gamma_R^2(o) = 30.6 \text{ mb}. \quad (20)$$

We parametrize

$$\gamma_i^2(t) = \gamma_i^2(0)\, e^{\frac{1}{2} b_i(t)} \text{ and choose } b_P = b_R = b_0,$$

with $b_0 = 8.3$ GeV^{-2}.[13]

III. SUM RULES

At large $M_x^2 >> M_N^2$ and $s/M_x^2 >> 1$, the cross section for inclusive process $a + b \to c + X$ can be expressed in terms of triple Regge contributions:

$$\frac{d\sigma}{dt dM_x^2} = \sum_{ijk} G_{ijk}(t)\, s^{\alpha_i(t)+\alpha_j(t)-2} (M_x^2)^{\alpha_k(0)-\alpha_i(t)-\alpha_j(t)} , \qquad (21)$$

where $$G_{ijk}(t) = \gamma_{aci}(t)\gamma_{acj}(t)\, X_i^*(t)\, X_j(t)\, g_{ijk}(t) \mathrm{Im} X_k(0) \gamma_{bbk}(0),$$

and $g_{ijk}(t)$ is the triple Regge coupling.

In the special case of $pp \to Xp$ under consideration with $a = b = c = p$ possible exchanges include P, f, ω, ρ, A_2 and π Regge poles which are known to couple to $N\bar{N}$. Let us look at these terms in more detail. Isospin and G-parity reduce the number of possible triple couplings

(i) In the PPR and PRP only PPf and PfP are permitted.

(ii) In RRP only ffP, $\omega\omega$P, $\pi\pi$P, $\rho\rho$P, A_2A_2P and $A_2\pi$P are possible. If we neglect also ρ and A_2 weakly coupled with $N\bar{N}$, then

RRP = ffP, $\omega\omega$P, and $\pi\pi$P

and PRR = Pff, fPf, P$\omega\omega$, ωPω.

The term P$\pi\pi$ vanishes due to spin-parity and the condition that $t = 0$ at the k-leg in the triple Regge diagram.

(iii) For RRR neglecting ρ and A_2 we have due to isospin and G-selection only RRR = fff, $\omega\omega$f, and $\pi\pi$f terms.

Again f$\pi\pi$ and πfπ are eliminated by spin-parity and f$\omega\omega$ + ωfω by exchange degeneracy of ω and f trajectories.

One could go further and assume degeneracy of the all triple couplings involving ω and f trajectories; however, this strong form of the exchange degeneracy which leads to cancellation of all off-diagonal terms is wrong in general[15] because ωPP and PωP terms which are partners of fPP and PfP vanish by G-parity. The other, weaker form of exchange degeneracy has been suggested in Ref. 16 for only terms with $k \neq P$. Then the term $PRR = Pff + fPf + P\omega\omega + \omega P\omega$ must vanish and the other ω couplings can be expressed in terms of the f coupling

$$
\begin{aligned}
G_{ffP} + G_{\omega\omega P} &= [\gamma_{acf}(t)]^2 \gamma_{bbP}(0)\, g_{ffP}(t) \frac{4}{\sin^2 \pi\alpha_R(t)} \\
G_{fff} + G_{\omega\omega f} &= [\gamma_{acf}(t)]^2 \gamma_{bbf}(0)\, g_{fff}(t) \frac{4}{\sin^2 \pi\alpha_R(t)} .
\end{aligned}
\tag{22}
$$

The arguments for this "weak" form of exchange degeneracy are based on the assumption of the normal two-component duality for nondiffractive terms of Eq. (21). However, as we shall see in the next section, application of our model to $pp \to Xp$ rules out the normal duality for nondiffractive terms. Thus we are left with all 6 unknown functions G_{ijk} entering the expression (21) plus two π-meson terms which we shall consider separately.

The high and low M_x behavior of inclusive cross section can be connected by finite mass sum rules.[5]

$$
\int_0^{\nu_0} d\nu\, \nu^n \left[\frac{d\sigma}{dtdM_x^2}(ab \to cX) + (-1)^{n+1} \frac{d\sigma}{dtdM_x^2}(cb \to aX)\right] = \sum_{ijk} G_{ijk}(t)\, \frac{s^{\alpha_i(t)+\alpha_j(t)-2}\, \nu_0^{\alpha_k(0)+n+1-\alpha_i(t)-\alpha_j(t)}}{\alpha_k(0)+n+1-\alpha_i(t)-\alpha_j(t)} , \tag{23}
$$

where $\nu = M_x^2 - M_N^2 - t$.

We shall use the first moment ($n = 1$) sum rules and saturate the low-energy integral with elastic and DHD-contributions, considered in the previous section. Then, in accordance with their s-dependence, the contributions into low- and high-mass parts of the sum rules can be separated into three relations, shown graphically in Fig. 3:

$$\langle E_{PP}\rangle + \langle D_{PP}\rangle = G_{PPP}\,\frac{\nu_0^{\alpha_P(0)+2-2\alpha_P(t)}}{\alpha_P(0)+2-2\alpha_P(t)} + G_{PPR}\,\frac{\nu_0^{\alpha_R(0)+2-2\alpha_P(t)}}{\alpha_R(0)+2-2\alpha_P(t)}$$

$$\langle E_{PR}\rangle + \langle D_{PR}\rangle = G_{PRP}\,\frac{\nu_0^{\alpha_P(0)+2-\alpha_P(t)-\alpha_R(t)}}{\alpha_P(0)+2-\alpha_P(t)-\alpha_R(t)} + G_{PRR}\,\frac{\nu_0^{\alpha_R(0)+2-\alpha_P(t)-\alpha_R(t)}}{\alpha_R(0)+2-\alpha_P(t)-\alpha_R(t)}$$

$$\langle E_{RR}\rangle + \langle D_{RR}\rangle = G_{RRP}\,\frac{\nu_0^{\alpha_P(0)+2-2\alpha_R(t)}}{\alpha_P(0)+2-2\alpha_R(t)} + G_{RRR}\,\frac{\nu_0^{\alpha_R(0)+2-2\alpha_R(t)}}{\alpha_R(0)+2-2\alpha_R(t)}\,. \qquad (24)$$

In principal one can write down the sum rules also for π-meson contributions but the closeness of the pion pole to the physical region permits us to estimate its contribution directly in terms of πN total cross section:[17]

$$G_{\pi\pi i}(t) = \frac{1}{4\pi}\,\frac{g^2_{\pi Np}}{4\pi}\,\sigma^i_{tot}(\pi p)\,\frac{(-t)e^{b_\pi(t-\mu^2)}}{(t-\mu^2)^2}\,, \qquad (25)$$

where $i = P$ and R and σ^P_{tot} and σ^R_{tot} are diffractive and nondiffractive contributions into total πN cross section (6) and $\exp[b_\pi(t-\mu^2)]$ is an off-shell form-factor.

The contributions of the elastic and the DHD amplitudes into low mass integral can be obtained using the result of Section III:

$$\langle E_{ij}\rangle = -t\,E_{ij}\,, \qquad (26)$$

and

$$\langle D_{ij}\rangle = D_{ij}\,Q(t), \qquad (27)$$

where

$$Q(t) \equiv \int_{\nu_{th}}^{\nu_0} \nu\, d\nu \left(\frac{d\sigma}{dt\,dM_x^2}\right)_0 \qquad (28)$$

Using the results of Ref. 3 this last integral was calculated. At small $|t|$ it can be approximated as $Q(t) \simeq 9\,e^{5.3t}$. Thus expression (24) gives us three equations which can be used to reduce the total number of 6 unknown triple Regge couplings to 3.

IV. ESTIMATION OF THE TRIPLE REGGE COUPLINGS

In this section we shall discuss some applications of the Eqs. (24). We shall examine cases of normal and abnormal duality for diffractive and non-diffractive terms and estimate triple Regge couplings for these cases.

Let us start from the two last equations (24) for nondiffractive terms. In the case of normal two-component duality we can split these equations and obtain the following expressions for nondiffractive triple couplings:

$$G_{PRR}(t) = \frac{1-(\alpha'_P+\alpha'_R)t}{\nu_0^{1-(\alpha'_P+\alpha'_R)t}} \langle E_{PR} \rangle \tag{29a}$$

$$G_{PRP}(t) = \frac{1.5-(\alpha'_P+\alpha'_R)t}{\nu_0^{1.5-(\alpha'_P+\alpha'_R)t}} \langle D_{PR} \rangle \tag{29b}$$

$$G_{RRR}(t) = \frac{1.5-2\alpha'_R t}{\nu_0^{1.5-2\alpha'_R t}} \langle E_{RR} \rangle \tag{29c}$$

$$G_{RRP}(t) = \frac{2(1-\alpha'_R t)}{\nu_0^{2-2\alpha'_R t}} \langle D_{RR} \rangle .$$

At small $|t|$ $G_{PRR}(t)$ is very small and negligible. The other triple couplings are shown in Fig. 6. In the case of abnormal duality the expressions for G_{ijk} will be the same, but with E_{ij} and D_{ij} interchanged. In this case $G_{PRP}(t)$

is negligible and the others are shown in Fig. 6 by dashed lines. We want to stress that in both cases the cross terms are very large.[18]

Let us consider now diffractive terms. In the previous calculations[19] based on the simple version of this approach, all nondiffractive terms were neglected. Guided by an approximate M_x^{-2} dependence of the experimental $pd \to Xd$ cross section, it was also suggested that the G_{PPR} is small and negligible. Then the steep t-dependence of the DHD contribution combines in (24) with vanishing at $t \to 0$ $\langle E_{PP}(t)\rangle$ and leads to a moderate t-dependence for $G_{PPP}(t) \sim 4{,}3\, e^{2,2t}$.[19] In the present case when secondary contributions are taken into account the relative value of the DHD term decreases and as a result $G_{PPP}(t)$ becomes more flat (see curve 1 in Fig. 7). The other cases shown in Fig. 7 are the following:

(2) normal duality:

$$G_{PPP}(t) = \frac{1 - 2\alpha'_P t}{\nu_0^{1 - 2\alpha'_P t}} \langle D_{PP}\rangle$$

$$G_{PPR}(t) = \frac{0.5 - 2\alpha'_P t}{\nu_0^{0.5 - 2\alpha'_P t}} \langle E_{PP}\rangle . \tag{30}$$

(3) abnormal duality [interchange of E_{ij} and D_{ij} in (30)].

(4) as an example we also show some particular case of mixed duality:

$$G_{PPP} = \epsilon_1 \langle E_{PP}\rangle + \epsilon_2 \langle D_{pp}\rangle$$

$$G_{PPR} = (1 - \epsilon_1)\langle E_{PP}\rangle + (1 - \epsilon_2)\langle D_{PP}\rangle ,$$

with $\epsilon_1 = 0.5$ and $\epsilon_2 = 1$.

Now we are ready for comparison with data. We shall restrict this comparison by special case of $t \to 0$[6] where the relations are especially simple. Even this restricted consideration will show us that extreme duality does not lead to agreement with data in the wide range of M_x^2/S from 0.01 to 0.1. For comparison we shall use the extrapolation[22] to $t = 0$ of the data on $pd \to Xd$[9b] and $pp \to Xp$.[15] This extrapolation introduces some uncertainty due to the experimental variation of the slope but we do not expect the effect to be large. The other problem is connected with difference in targets and includes:

(a) Deuteron structure. We shall use the reduction of the deuteron data to the nucleon cross section by dividing out the deuteron form factor as was done in Ref. 9b.

(b) Different quantum numbers and consequently different exchanges. Since ρ and A_2 contributions are small, the main difference comes from π-exchange. In fact, π does not contribute at $t = 0$, but the cross section at $t \neq 0$ used in the extrapolation (Ref. 22) has the π contribution. The estimation of this effect is shown in Fig. 8. Crossed points are the result of the extrapolation from $t = -0.2\ \text{GeV}^2$ of the nucleon cross section from which $\pi\pi P$ and $\pi\pi R$ terms[25] were subtracted.

Curve 1 in Fig. 8 shows the contribution of the nondiffractive terms in the normal case. One can see that this contribution is very large. Since the rest (diffractive) contributions are non negative, we can conclude that this case is positively ruled out. At the same time nondiffractive contributions in the abnormal case are relatively small and vary between $0.6\ \text{mb} \cdot \text{GeV}^{-2}$

at $M_x^2/s = 0.01$ and $1.1\ \mathrm{mb} \cdot \mathrm{GeV}^{-2}$ for $M_x^2/s = 0.1$. Diffractive contributions in a normal case in combination with abnormal nondiffractive terms are shown by curve 2 which is close to the experimental points but too flat. At the same time the abnormal diffractive term is in apparent disagreement with data (curve 3).

We can give up the normal duality for the cross nondiffractive terms, connected with $R + N \to P + N$ scattering, maintaining it for $R + N \to R + N$. The nondiffractive contributions in this case are shown by curve 1 in Fig. 9, and the whole cross section for abnormal and normal diffractive terms--by curves 2 and 3 correspondingly. Both these curves are in disagreement with data, although curve 3 is closer.

Figure 10 shows the comparison with data for the case of normal cross terms ij = RP and abnormal ij = RR. Abnormal diffractive terms lead to curve 2 which is close to data while normal disagrees (curve 3).

All the cases are summarized in Table I, where "Norm" and "Ab" mean normal and abnormal two-component duality. A plus in the last column indicates closeness of the predicted results to the data, while a minus shows apparent disagreement.

Table I.

	RR	PR	PP	
Fig. 8	Norm	Norm	Norm	-
	Norm	Norm	Ab	-
	Ab	Ab	Norm	+
	Ab	Ab	Ab	-
Fig. 9	Norm	Ab	Norm	+
	Norm	Ab	Ab	-
Fig. 10	Ab	Norm	Norm	-
	Ab	Norm	Ab	+

Even for those cases where curves are close to the experimental points they still do not give good description for the whole M_x^2/s-interval considered. Thus we can conclude that extreme two-component duality for diffractive and nondiffractive terms is in contradiction with our model and experimental data on nucleon dissociation and mixed duality is needed at least for one or two Reggeon-particle amplitudes: $Ph \to Ph$, $Ph \to RH$, $Rh \to Rh$. The proper ratio of different contributions in this case can be obtained by using Eq. (24) together with fit of the data which will be done elsewhere. [Note that in contrast to the usual way of using FMSR in a fit program[23] Eq. (24) gives more detailed constraints on triple Regge terms.]

The other important conclusion is that irrespectively of diffractive terms normal duality is ruled out for the whole nondiffractive contribution although it is possible separately for RP or RR terms.

The vanishing of the triple Pomeron coupling G_{PPP} at $t \to 0$ is possible in our approach only in the case of extreme abnormal duality for $Pp \to Pp$ amplitude which seems to be unfavorable from our analysis.

ACKNOWLEDGMENTS

I am very grateful to M. Einhorn, G. Fox, G. L. Kane, S. Mukhin, and C. Quigg for useful discussion.

REFERENCES

[*] Joint Institute for Nuclear Research, Dubna, and P. N. Lebedev Physical Institute, Moscow, USSR

[†] Operated by Universities Research Association Inc. Under Contract with the United States Atomic Energy Commission.

[1] For review of the recent data see S. V. Mukhin and V. A. Tsarev. Invited paper presented at the 1974 Meeting of the Division of Particles and Fields of the APS, Williamsburg, Virginia.

[2] CERN-Hamburg-Orsay-Vienna Collaboration, E. Nagy et al., Paper submitted to the XVII International Conference on High Energy Physics, London, 1974.

[3] V. A. Tsarev, Fermilab-Pub-74/80-THY/EXP (1974).

[4] S. D. Drell and K. Hiida, Phys. Rev. Letters 7, 199 (1961); R. Deck, Phys. Rev. Letters 13, 1969 (1964).

[5] J. Kwiecinski, Nuovo Cimento 3, 619 (1972); A. I. Sanda, Phys. Rev. D6, 280 (1972); M. B. Einhorn, J. E. Ellis and J. Finkelstein, Phys. Rev. D5, 2063 (1972).

[6] Physical region for the M_x production is restricted by $|t| > |t_{min}|$ where $|t_{min}| \simeq (M_x^2 - M_n^2/2p)^2$. At large energies t_{min} is small and we shall neglect it.

[7] H. Harari, Phys. Rev. Letters 20, 1395 (1968); P. G. O. Freund, Phys. Rev. Letters 20, 235 (1968).

[8] For review see M. B. Einhorn, Proc. of the XVI International Conference on High Energy Physics, Batavia 1972, Vol. I, p. 417.

[9] P. Hoyer, Invited talk presented at the XVII International Conference on High Energy Physics, London, 1974.

[10] M. B. Einhorn, M. B. Green, and M. A. Virasoro, Phys. Letters 37B, 292 (1971).

[11] S. H. Tye and G. Veneziano, Phys. Letters 38B, 30 (1972).

[12] $b^{o}_{\pi N}$ is an energy-independent part of the πN-slope. The value 9 GeV^{-2} chosen in Ref. 3 for the total slope at $s \sim 400$ GeV^2 is equivalent to $b_{\pi N} = b^{o}_{\pi N} + 2\alpha'_P \ln s$ with $\alpha'_P \simeq 0.25$ GeV^{-2}.[13]

[13] B. Bartenev et al., Phys. Rev. Letters 31, 1088 (1973).

[14] (a) E. W. Anderson et al., Phys. Rev. Letters 16, 854 (1966); R. M. Edelstein et al., Phys. Rev. D5, 1073 (1972).

(b) Y. Akimov et al., Fermilab-Conf-74/56-EXP (1974).

(c) B. Bartenev et al., Phys. Letters B51, 299 (1974).

(d) Y. Akimov et al., Fermilab-Conf-74/79-EXP (1974).

[15] R. Shankar preprint LBL-2678 (1974).

[16] L. A. P. Balazs, Fermilab-Pub-74/78-THY (1974).

[17] M. Bishari, Phys. Letters 38B, 510 (1972) and LBL-2066 (1973).

[18] The fact that the Deck-type model predicts large cross triple Regge terms was also pointed out for the case of π-dissociation by G. Fox, Proc. of International Conference on High Energy Collisions, Stony Brook, 1973.

[19] Y. Akimov et al., Fermilab-Conf-74/79-THY/EXP (1974).

[20] We take here into account the different definition of the G_{PPP} in Ref. 19: $G_{PPP} = G_{PPP}\,(\text{Ref. } 19)\, \exp[-2\alpha'_P\,(1 + \ln \bar{s}/\nu_o)]\,t$. $\bar{s} \simeq 2M_d\bar{p} \simeq 1000$ GeV^2.

[21] CERN-Holland-Lancaster-Manchester Collaboration, Albrow et al., data presented in Ref. 22.

[22]F. K. Loebinger, Review talk presented at the XVII International Conference on High Energy Physics, London, 1974.

[23]D. P. Roy and R. G. Roberts, Rutherford Laboratory preprint RL-74-022 T79 (1974); R. D. Field and G. C. Fox, CALT-68-434 (1974).

FIGURE CAPTIONS

Fig. 1. The mass spectrum for the $n\pi^+$ system.[2] The resonance peaks are clearly seen in the backward Jackson hemisphere. The area under these peaks is much smaller than the sum of areas of non-resonant bumps in the forward and backward Jackson hemispheres.

Fig. 2. The pion-triangle model for triple Regge coupling.

Fig. 3. Graphical representation of the sum rules.

Fig. 4. Drell-Hiida-Deck-type diagrams for $pp \rightarrow \pi Np$.

Fig. 5. Energy dependence of the 1.4 GeV bump in the proton dissociation.

Fig. 6. Nondiffractive triple Regge couplings.

Fig. 7. Diffractive triple Regge couplings.

Fig. 8. Comparison with experiment. 1- normal nondiffractive contributions. 2- abnormal nondiffractive + normal diffractive. 3- abnormal nondiffractive + abnormal diffractive.

Fig. 9. Comparison with experiment. 1- nondiffractive contributions, RR-normal, PR-abnormal. 2- (1) + abnormal diffractive. 3- (1) + normal diffractive.

Fig. 10. Comparison with experiment. 1- nondiffractive contributions PR-normal, RR-abnormal. 2- (1) + abnormal diffractive. 3- (1) + normal diffractive.

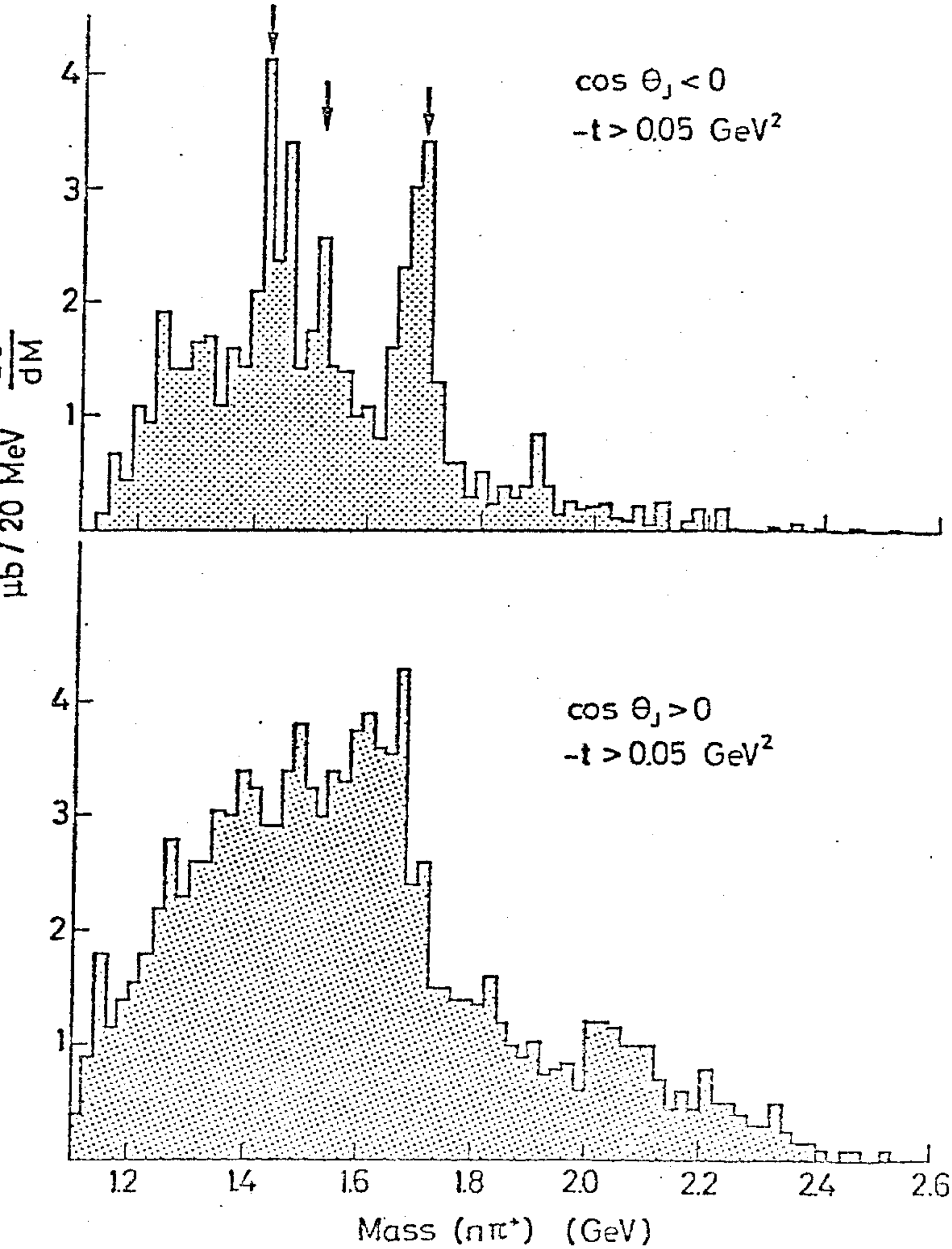
cos Θ_J < 0
-t > 0.05 GeV²
cos Θ_J > 0
-t > 0.05 GeV²
μb / 20 MeV dσ/dM
1
2
3
4
1.2
1.4
1.6
1.8
2.0
2.2
2.4
2.6
Mass (nπ⁺) (GeV)

Fig. 1

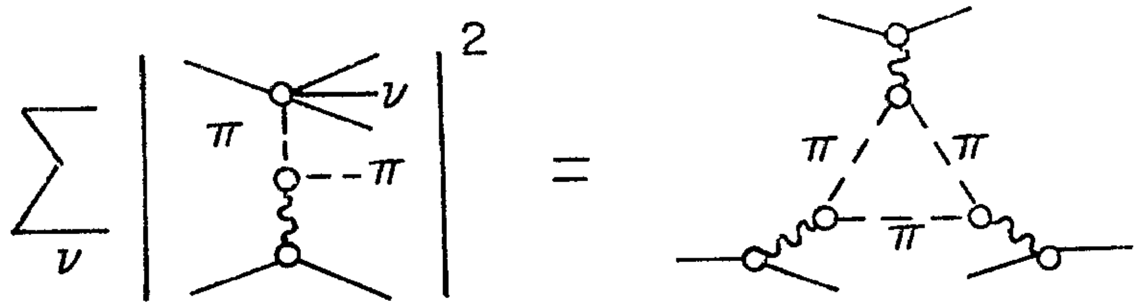

Fig. 2

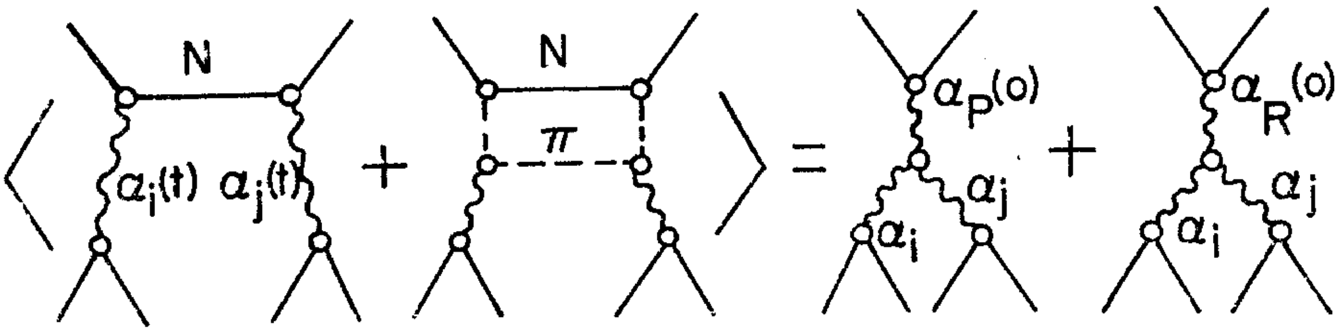

Fig. 3

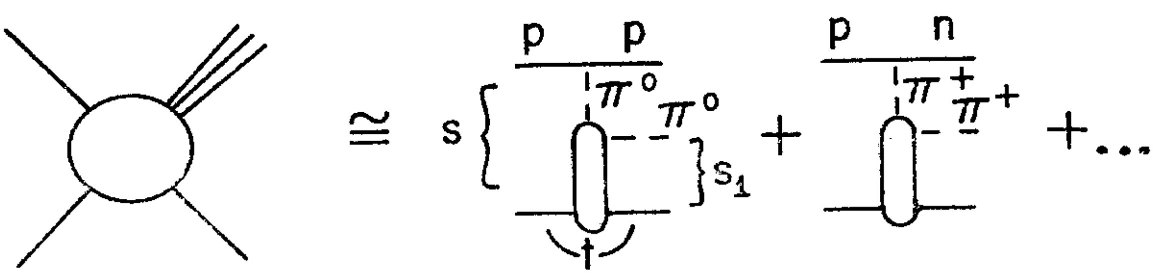

Fig. 4

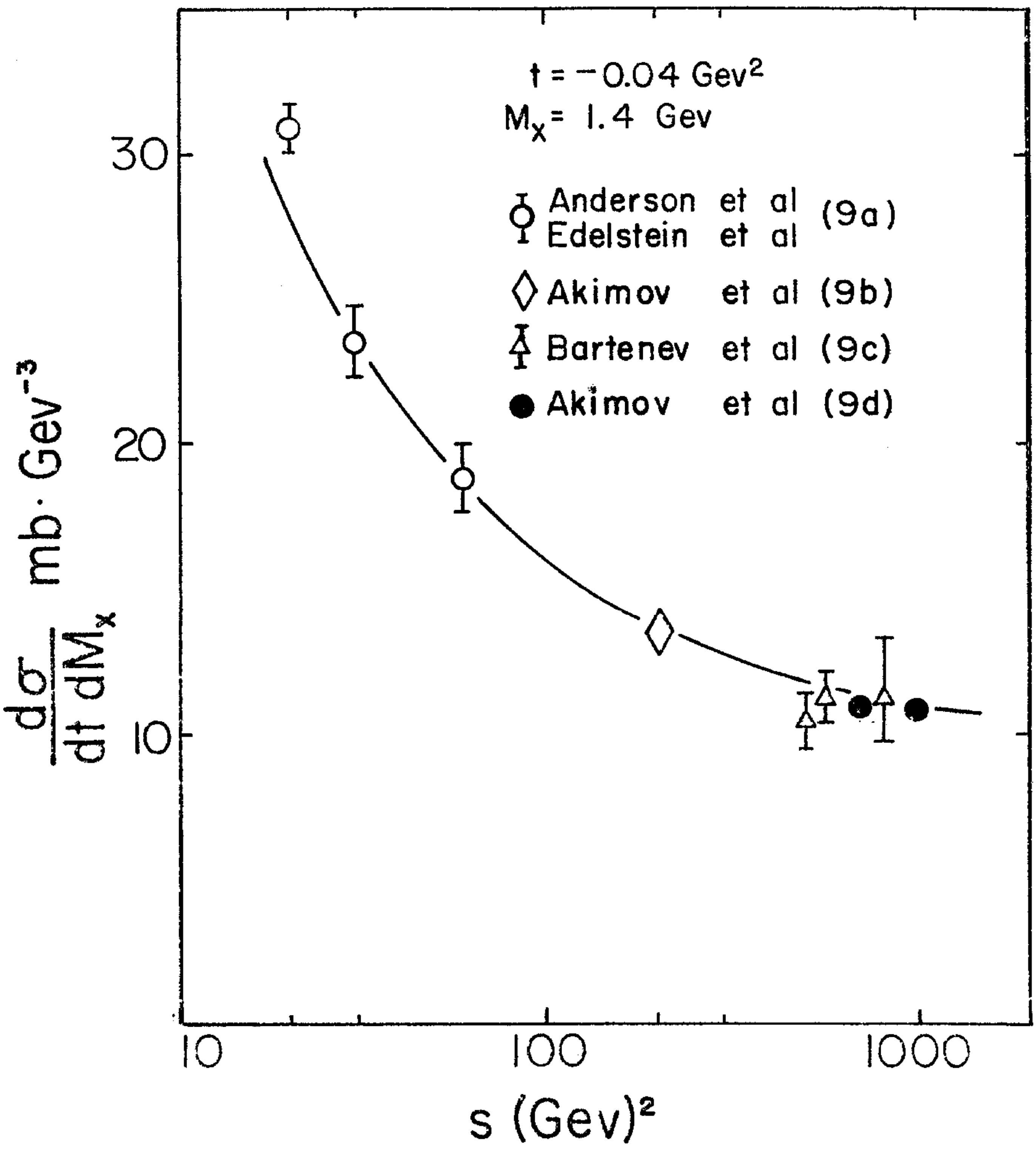
t = −0.04 Gev²
Mx= 1.4 Gev
Anderson et al
Edelstein et al (9a)
Akimov et al (9b)
Bartenev et al (9c)
Akimov et al (9d)
30
20
10
10
100
1000
s (Gev)²
dσ/dt dMx mb · Gev⁻³

Fig. 5

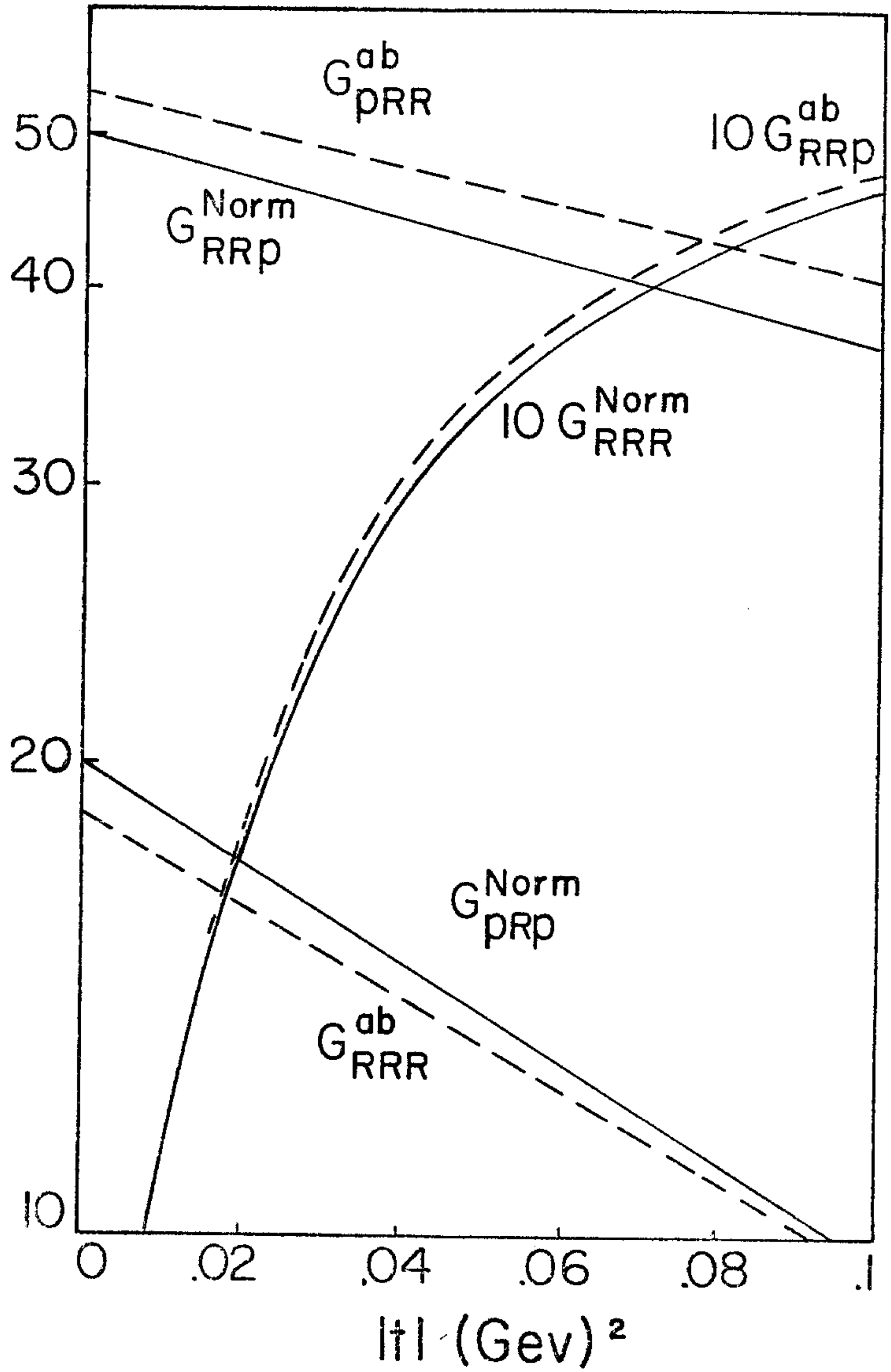

G^{ab}_{pRR}
$10\,G^{ab}_{RRp}$
50
G^{Norm}_{RRp}
40
$10\,G^{Norm}_{RRR}$
30
20
G^{Norm}_{pRp}
G^{ab}_{RRR}
10
0
.02
.04
.06
.08
.1
|t| (Gev)²

Fig. 6

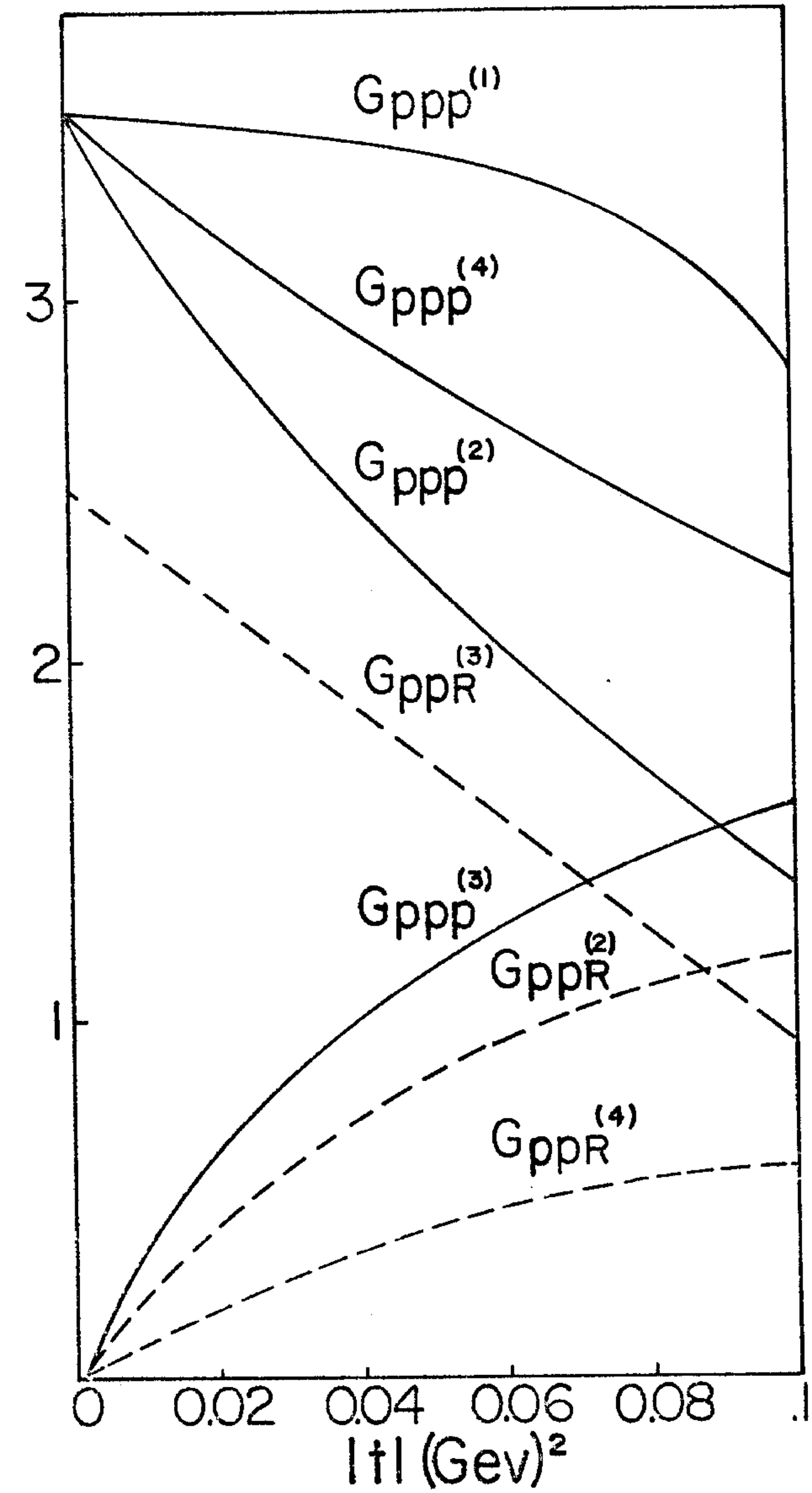

$G_{ppp}^{(1)}$
$G_{ppp}^{(4)}$
$G_{ppp}^{(2)}$
$G_{ppR}^{(3)}$
$G_{ppp}^{(3)}$
$G_{ppR}^{(2)}$
$G_{ppR}^{(4)}$
3
2
1
0
0.02
0.04
0.06
0.08
.1
|t| (Gev)^2

Fig. 7

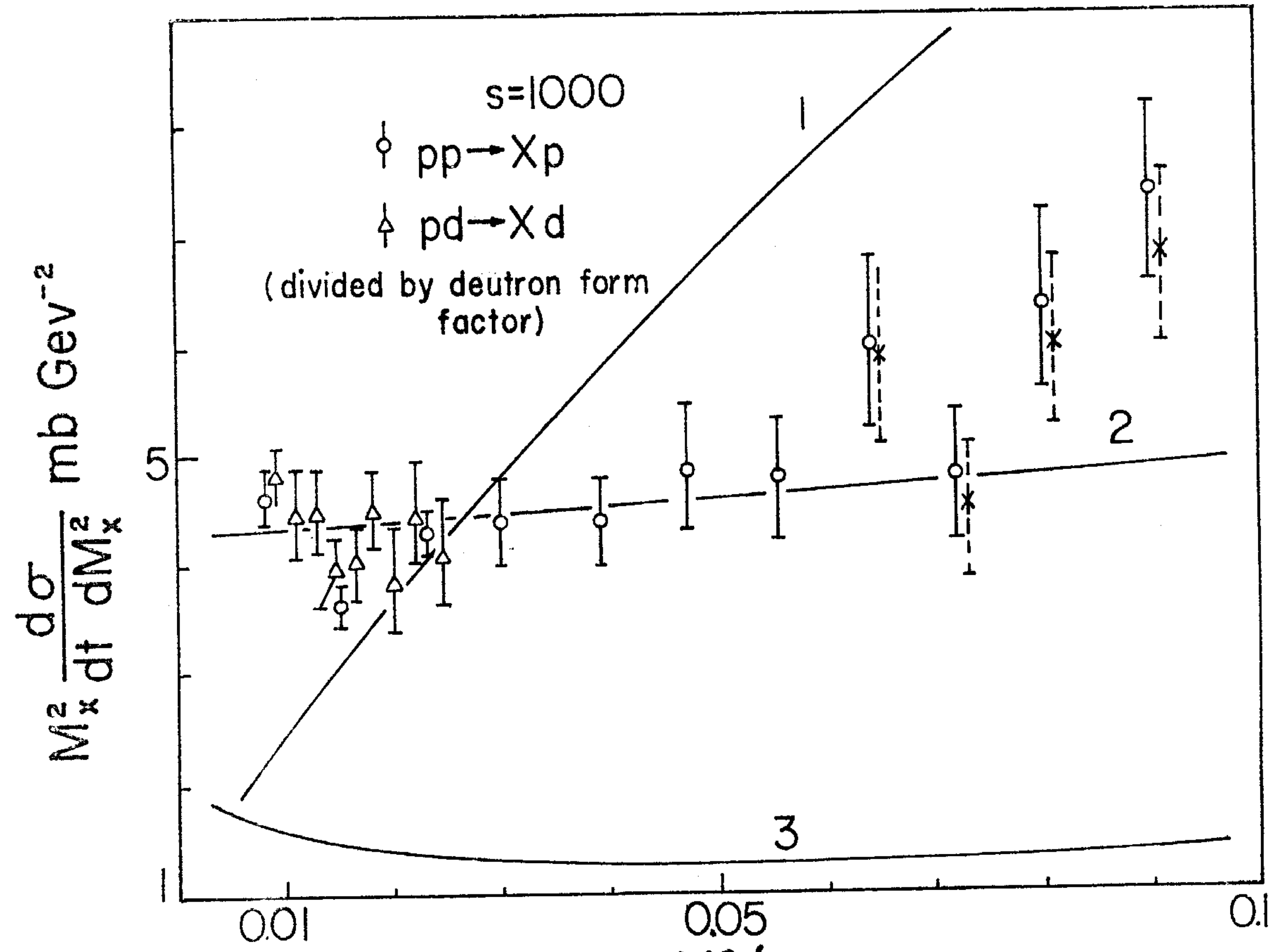

s=1000
pp → Xp
pd → Xd
(divided by deutron form factor)
1
2
3
5
1
0.01
0.05
0.1
M_x^2/s
$M_x^2 \frac{d\sigma}{dt\, dM_x^2}$ mb Gev^{-2}

Fig. 8

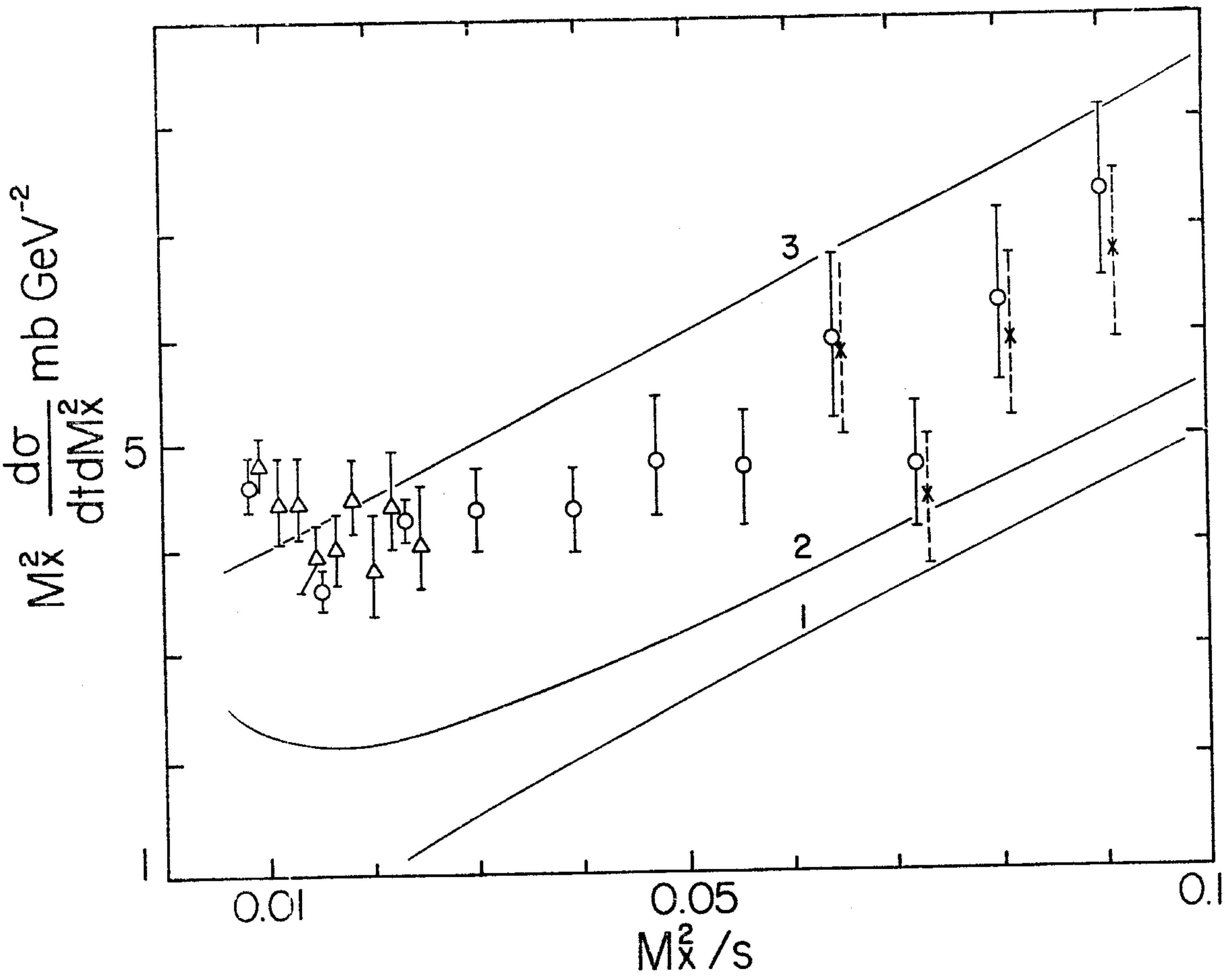

Fig. 9

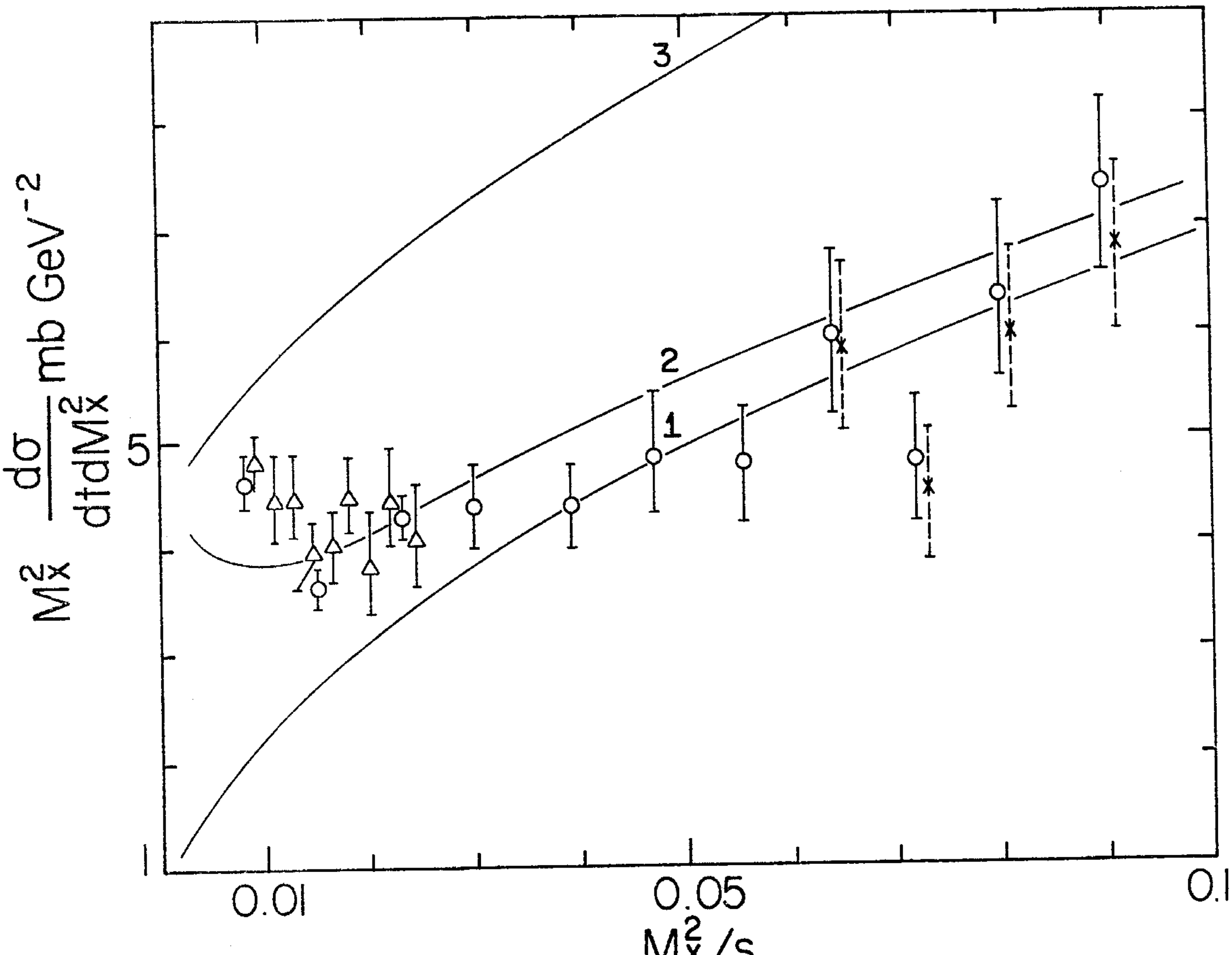

Fig. 10